Predator Persistence through Variability of Resource Productivity in Tritrophic Systems

Soudijn, F.H.; de Roos, A.M.

Published in:
American Naturalist

DOI:
10.1086/694119

 DOI: 10.1086/694119

Appendix from F. H. Soudijn and A. M. de Roos, "Predator Persistence through Variability of Resource Productivity in Tritrophic Systems" (Am. Nat., vol. 190, no. 6, p. 000)

Part A. Model Description

Model Details

To study the effect of variability on the trophic transfer efficiency, we use a model system with three trophic levels of an unstructured resource, a size-structured consumer, and an unstructured size-specific predator. The consumer population is represented by a stage-structured biomass model that distinguishes juvenile and adult consumers, as described by de Roos et al. (2008*b*). The model has been described and extensively used previously (de Roos et al. 2008*a*; Ohlberger et al. 2011; de Roos and Persson 2013). Here, we follow the notation described by de Roos and Persson (2013). A summary of the equations and parameter values can be found in tables A1 and A2, respectively. Below is a detailed description of the model assumptions.

The stage-structured biomass has been derived as an approximation to a model accounting for a complete size distribution of juveniles and a class of nongrowing adult individuals (de Roos et al. 2008*b*). The stage-structured biomass model is, moreover, mathematically identical to its continuously size-structured analogue under equilibrium conditions. Individuals are assumed to be born with the same size and mature at the same size. The stage-structured biomass model and its size-structured analogue follow the bioenergetics approach introduced by Yodzis and Innes (1992), in which net biomass production is the balance between assimilated energy and maintenance. While juveniles invest all their energy in growth, adults are assumed to invest all their energy in reproduction. All energetic rates are assumed to scale proportionally with individual body size. Henceforth, we will continue the model description in terms of mass-specific rates for energy acquisition and use. Despite a lower mass-specific ingestion rate for adults, the ingestion of an adult individual may nonetheless be larger than juvenile ingestion due to the larger adult body size.

Adults A and juveniles J share a common resource R. Food ingestion for juveniles and adults follows a Holling type II functional response as a function of resource density (table A1). The parameter q modulates the maximum ingestion rate of juveniles and adults; it represents differences in ingestion between life stages in a phenomenological way (Persson and de Roos 2013). For $q < 1$, juveniles are better at ingesting the resource and have a competitive advantage over adults. For values of q higher than 1, the opposite holds.

After assimilation, ingested food is first used to cover the mass-specific somatic maintenance costs (table A1). When the assimilated energy exceeds the maintenance costs, the net energy production is invested in growth in the juvenile stage and in reproduction in the adult stage. If the assimilated energy is not sufficient to balance the maintenance costs, biomass is lost due to starvation. Under starvation conditions, somatic growth and, hence, maturation stops, and no energy is invested in reproduction.

Both juveniles and adults suffer from mortality (table A1). The mortality rates are a summation of background mortality, predation mortality, and starvation. When juveniles starve, the loss rate from the juvenile stage therefore equals $(\nu_J(R) - \mu_C)J$, where $\nu_J(R)$ is the mass-specific net energy production rate of juveniles, which is negative under starvation conditions. When adults starve, the loss rate from the adult stage equals $(\nu_A(R) - d_A(P))A$, where $\nu_A(R)$ is the mass-specific net energy production rate of adults, which is negative under starvation conditions.

The function for the mass-specific maturation rate translates the individual-level assumptions about energy expenditure into a population-level maturation rate. It is, in fact, the functional form of the maturation rate, which guarantees that the stage-structured biomass model under equilibrium conditions is identical to its underlying, fully size structured analogue (see the derivation in de Roos et al. 2008*b*). Maturation occurs when individuals reach a specific body size, and the maturation rate depends on the ratio between the size at birth and the size at maturation (table A1). Maturation is restricted to positive values of the mass-specific net energy production of juveniles ν_J and depends on the juvenile mortality rate. The function approaches 0 for $\nu_J \downarrow 0$ and never reaches negative values, while it has a regular limit equal to $-\mu_C/\ln(z)$ for $\nu_J \to \mu_J$ (de Roos et al. 2008*b*).

In the absence of consumers, the resource follows semichemostat growth with sinusoidal fluctuations in the resource growth (table A1). When consumers are present, the resource biomass declines through food ingestion by consumers.

The predator is assumed to forage on adult consumers only, and food intake by predators follows a type II functional response (table A1). The predator P dynamics also follow bioenergetic assumptions (Yodzis and Innes 1992). The ingested food is first used to cover maintenance requirements. When the ingested food is not sufficient to cover maintenance costs, predators suffer from starvation mortality. In addition, predators suffer from background mortality.

Parameter Derivation

Parameterization is based on scaling relationships with average adult body size, following the approach laid out by de Roos and Persson (2013, boxes 3.4, 4.2). The model was parameterized for an invertebrate consumer and a predator with an average adult body mass (wet weight) of 0.0001 and 0.01 g, respectively. Default parameter values can be found in table A2. The mass-specific ingestion rate of juvenile and adult consumers differs by a factor q that, hence, controls the competitive difference between life stages. Its value is chosen such that adults always have a competitive advantage over juveniles (table A2).

Computational Techniques

Time dynamics of the model with the stage-structured consumer were computed with numerical integrations of the system of ordinary differential equations using C-based software. For all parameter values we studied, these numerical simulations showed that dynamics converged to stable cycles with a period identical to the period of productivity fluctuations Y (see fig. 1). Parameter dependencies of these cycles were studied by numerical continuation techniques of the curves representing the resource, the juvenile and adult consumers, and the predator biomass densities at the beginning of the cycle as a function of the parameter Y, the amplitude of the productivity fluctuations ψ, and μ_P, the mortality of the predator population. While calculating the parameter dependence of the dynamics, we also computed average densities over the cycles with period Y of the resource, consumer stages, and predator in relation to Y, ψ, and μ_P. The boundaries in parameter space of predator persistence were computed by analyzing for which parameter values the growth rate of the predator was 0 for a situation without predation feedback of the predator on the prey. The curve of the equilibrium predator density as a function of the predator mortality is folded (see "Results" in the main text, fig. 3), resulting in two limit points in the curve. The location of these limit points in parameter space was determined by finding the parameter values for which the tangent along the curve of biomass densities of the variables at the beginning of the cycle with period Y in relation to the parameters is vertical. Continuation of the biomass cycles, localization of the predator persistence point, and localization of the limit points were determined using a publicly available software package that allows for the computation of solutions to generic systems of nonlinear equations as a function of parameters (https://bitbucket.org/amderoos/findcurve). The source code, header file, and R scripts necessary to produce figures 2*A*, 2*C*, 3, and A1 in this article are included in a zip file.[1]

Stochastic Fluctuations in Resource Productivity

To test the robustness of our results to stochastic variability in resource productivity, we use the model as described in the main text with stochastic daily variation instead of sinusoidal fluctuations in the productivity of the resource. Spectral synthesis and spectral mimicry methods as described previously by Vasseur (2007) were used to generate stochastic, day-to-day variation in the maximum resource density $R_{\max}$. The power spectrum of the stochastic time series of $R_{\max}$ values scales as $1/f^{\beta}$. The color of the stochastic variation is determined by parameter β; we tested the effect of pink ($\beta = 0.5$) noise on the predator-prey dynamics. The mean value of $R_{\max}$ was kept equal to the default value (table A2). We varied the value of the coefficient of variation (CV) of the stochastic variability in the values for $R_{\max}$ to investigate the effect of increasing variability on the dynamics. The range of values for the CV tested were limited to values that always generated positive values for $R_{\max}$. Model dynamics were studied using numerical integrations of the system of ordinary differential equations presented in table A1 but with regular semichemostat growth for the resource productivity term:

$$G(R) = \rho(R_{\max} - R). \tag{A1}$$

[1] Code that appears in *The American Naturalist* is provided as a convenience to the readers. It has not necessarily been tested as part of the peer review.

To assess dependence of the dynamics on the CV of the stochastic variability, model integrations were simulated over long time periods while varying the value of the CV in small steps every 50,000 time units (for an explanation of this procedure to study parameter dependence of model results, see de Roos and Persson 2013, box 3.5). Average values were calculated in such bifurcation runs over the last 60% of the 50,000 time steps.

Table A1: Model equations and functions of the stage-structured biomass model

Equation or function	Description
$\frac{dR}{dt} = G(R) - \omega_J(R)J - \omega_A(R)A$	Resource biomass dynamics
$\frac{dJ}{dt} = v_A^+(R)A + v_J(R)J - \gamma(v_J(R), \mu_C)J - \mu_C J$	Juvenile consumer biomass dynamics
$\frac{dA}{dt} = \gamma(v_J(R), \mu_C)J + (v_A(R) - v_A^+(R))A - d_A(P)A$	Adult consumer biomass dynamics
$\frac{dP}{dt} = (v_P(A) - \mu_P)P$	Predator biomass dynamics
$G(R) = \rho R_{\max}\left(1 + \psi \sin\left(2\pi \frac{t}{Y}\right)\right) - \rho R$	Resource growth rate
$\omega_J(R) = (2 - q)M_C \frac{R}{H_C + R}$	Mass-specific resource ingestion rate, juvenile consumers
$\omega_A(R) = q M_C \frac{R}{H_C + R}$	Mass-specific resource ingestion rate, adult consumers
$v_J(R) = \sigma_C \omega_J(R) - T_C$	Mass-specific juvenile consumer net energy production rate
$v_A(R) = \sigma_C \omega_A(R) - T_C$	Mass-specific adult consumer net energy production rate
$d_A(P) = \mu_C + M_P \frac{P}{H_P + A}$	Adult consumer mortality rate
$\gamma(v_J^+(R), \mu_C) = \begin{cases} \frac{(v_J(R) - \mu_C)}{(1 - z^{1-\mu_C/v_J(R)})} & \text{if } v_J(R) > 0 \\ 0 & \text{if } v_J(R) \le 0 \end{cases}$	Mass-specific juvenile consumer maturation rate
$v_P(A) = \sigma_P M_P \frac{A}{H_P + R} - T_P$	Predator net biomass production rate per unit of biomass

Note: The mass-specific net biomass production restricted to positive values of adults is represented by $v_A^+(R)$.

Table A2: Model parameters and variables and default parameter values of the stage-structured biomass model

Symbol	Unit	Description	Value
Variables:			
R	mg L^{-1}	Consumer resource	...
J	mg L^{-1}	Juvenile consumer biomass	...
A	mg L^{-1}	Adult consumer biomass	...
P	mg L^{-1}	Predator biomass	...
Resource:			
R_{max}	mg L^{-1}	Maximum biomass density	40.0
ρ	day^{-1}	Turnover rate	.1
Y	days	Period of fluctuations	10.0
ψ	...	Proportionality constant amplitude of fluctuations	0–0.6
Consumer:			
M_C	day^{-1}	Mass-specific maximum ingestion rate	1.0
H_C	mg L^{-1}	Half-saturation resource density	3.0
T_C	day^{-1}	Mass-specific maintenance rate	.1
σ_C	...	Assimilation efficiency	.5
μ_C	day^{-1}	Background mortality rate	.015
z	...	Ratio of consumer body size at birth and maturation	.5
q	...	Competitive difference between stages	1.5
Predator:			
M_P	day^{-1}	Mass-specific maximum ingestion rate	.32
H_P	mg L^{-1}	Half-saturation resource density	3.0
T_P	day^{-1}	Mass-specific maintenance rate	.032
σ_P	...	Assimilation efficiency	.5
μ_P	day^{-1}	Background mortality rate	.005

Part B. Supplemental Figure

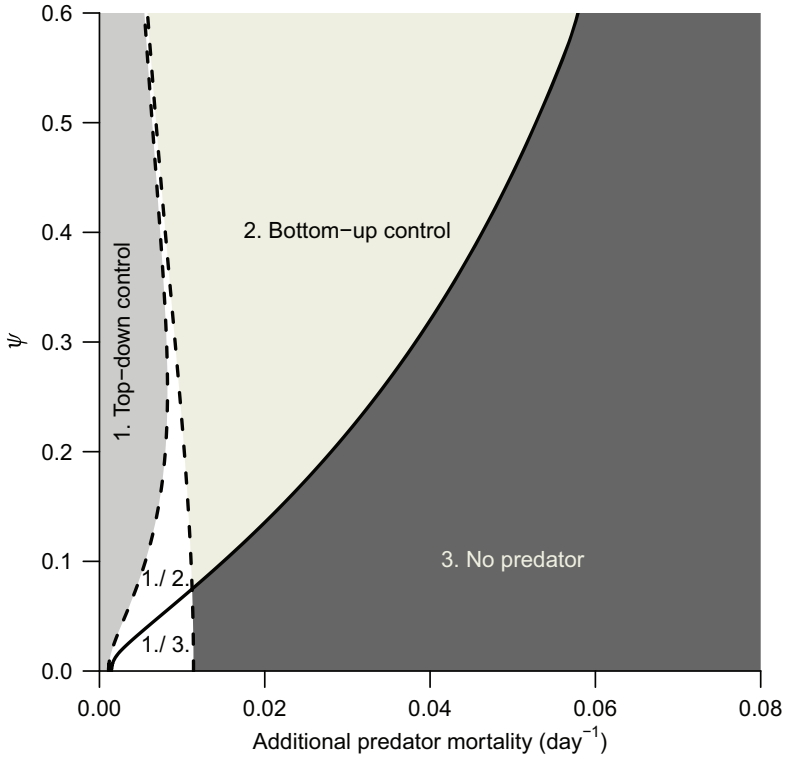

Figure A1: Boundaries of parameter regions with predator extinction (solid black line) and with the predator present, in which the dynamics are controlled either top-down by the predator or bottom-up (dashed black lines) as a function of the amplitude of resource productivity fluctuations ψ and predator mortality rate μ_P. Parameter domains with the predator and top-down (1, light gray) or bottom-up (2, ivory) control of the dynamics, zero predator density (3, dark gray), and bistability (white) are indicated in the plot. The region with alternative stable dynamics is divided into a region of bistability between top-down control of the dynamics by the predator and zero predator density (1./3.), below the extinction boundary of the predator, and a region of bistability between top-down control of the dynamics by the predator and dynamics with the predator present that are controlled bottom-up (1./2.), above the extinction boundary of the predator. Default parameter values (table A2) were used for the calculations.